Hindawi Publishing Corporation
Journal of Chemistry
Volume 2013, Article ID 274838, 10 pages
http://dx.doi.org/10.1155/2013/274838

Research Article

Investigation of the Orientation of CTA^+ Ions in the Interlayer of CTAB Pillared Montmorillonite

Semra Karaca,[1] Ahmet Gürses,[2] and Mehtap Ejder Korucu[1]

[1] *Department of Chemistry, Faculty of Science, Atatürk University, 25240 Erzurum, Turkey*
[2] *Department of Chemistry, K.K. Education Faculty, Atatürk University, 25240 Erzurum, Turkey*

Correspondence should be addressed to Semra Karaca; skaraca@atauni.edu.tr

Received 19 June 2012; Accepted 9 July 2012

Academic Editor: Huu Hao Ngo

The orientation of CTA^+ in the interlayer of organic pillared montmorillonite prepared by adding different amounts of surfactant corresponding to the CEC of the pristine clay mineral has been studied using X-ray diffraction (XRD), Fourier Transform Infrared (FTIR) spectra. Morphology of the samples was examined by scanning electron microscopy (SEM). The results are supported by the measurements of zeta potentials and contact angles of pristine clay and organoclay samples. From the XRD results, a series of arrangement models of CTA^+ in the interlayer of montmorillonite have been proposed as lateral-bilayer, pseudotrilayer, paraffin-type-monolayer and pseudotrilayer, paraffin-type-bilayer and pseudotrilayer for 0.5, 1, 1.5, and 2.0 CEC, respectively. FTIR spectrum and contact angle measurements of pristine montmorillonite and organoclays indicated the incorporation of surfactant and the changing of hydrophility in the different OMts. This study demonstrates that not only the arrangement model of surfactant, but also the morphology of organoclay strongly depends on the surfactant packing density within the montmorillonite interlayer space. In addition, it can be also proposed that, the magnitude of surface charge or its distribution on clay mineral might be an important factor for expansion characteristics of organoclay.

1. Introduction

Modification of clay mineral surfaces by adsorption of organic compounds has been largely studied in the literature. "Organoclay minerals" (also called "bentonite") were initially used for their rheological properties, but their most recent application is as filler for a polymer, in order to modify its mechanical, thermal, or barrier properties. Organomontmorillonites (OMts) have found wide applications in organic pollution control fields because of their excellent adsorption capacity towards hydrophobic organic compounds [1–6]. Understanding microstructure of this kind of organoclays is of high importance for clarifying their adsorption characteristics and improving their adsorption efficiency. In the past decades, structural characteristics of OMt have been extensively investigated. The structural characteristics, such as basal spacing, surface area, porous structure, and arrangement models of organic cations, have been reported in numerous publications [7–16]. Based on the obtained structural information, the potential correlation between microstructure and adsorption characteristics of organoclays has been proposed in several reports [1, 17–24]. Chen et al. [5] indicated that as the arrangement model of organic cations evolves from flat-monolayer to flat-bilayer, to pseudotrilayer, then to paraffin-monolayer and finally to paraffin-bilayer with the increase of their loading amounts, the alkyl chains will first form strong adsorbed organic film and then gradually transfer to weak partition organic phase.

For this purpose, smectites are the clay minerals mainly used after surfactant modification, as filler in clay-polymer nanocomposites [25]. The smectites are layered inorganic phyllosilicates where the layers of about 1 nm are held apart mainly by electrostatic forces. Montmorillonite is one of the most common smectites, which is widely used in a range of applications because of its high cation exchange capacity, swelling capacity, high surface areas, and resulting strong adsorption. There are two natural varieties of montmorillonite: sodium montmorillonite having a high swelling capacity in water and calcium montmorillonite with slight swelling capacity. The ability to cation exchange in the interlayer space

Table 1: The analysis of particle size of montmorillonite clay.

Clay amount (%)	ASTM particle size
50.942	>150 μm
23.346	150–106 μm
24.6	85–38 μm
0.634	<38 μm
0.462	106–85 μm

Table 2: XRF results of montmorillonite.

Component	%
SiO_2	59.32
Al_2O_3	17.19
Fe_2O_3	5.949
MgO	3.632
CaO	2.211
Na_2O	1.667
K_2O	0.9732
TiO_2	0.7436
SO_3	0.5068
Other	7.8074

determines the most interesting property of this material which can be used as a filler for nanocomposites showing unique mechanical properties [26]. Consequently, smectites have found many applications in the fields of cosmetic, catalysis, adsorption, and so forth. The general approach to improve the different mechanical and thermal properties involves the mixing of a polymer with traditional fillers like talc, glass fibers, calcium carbonate, and so forth. Recently, great efforts have been paid on synthesis and application of inorganic-organic clay complexes [27–31].Wu et al. [29] found that modifying inorganic pillared montmorillonites with surfactant could greatly improve their sorbing capacity to phenol. By preadsorption of organic molecules (amines) between the clay layers prior to pillaring with aluminium precursor, it was possible to increase the microporosity of the obtained materials [30]. However, up to now, there are few studies on the interlayer structure and surface properties of the importance for the synthesis and applications. The aim of this study is to investigate the microstructure of CTAB-Mt complexes and the effect resulted from the premodified surfactant loadings. This study provides some new insights in the synthesis of inorganic-organic clay complexes and the interlayer structure of the resulting materials. It is important for well understanding the structure and properties of inorganic-organic clays and their applications.

2. Materials and Methods

2.1. Material. Montmorillonite is used in this study, a commercial sample of bentonite of Çankırı deposit in Turkey was obtained from Karakaya A. Ş. Mineral Company, Ankara, Turkey. The sample was air-dried, sieved and distribution of particle size determined using ASTM Standard sieves. The results are given in Table 1. Chemical composition of the clay sample was determined by Rigaku RIX-3000 X-ray fluorescence spectrometry (Rigaku Corporation, Tokyo, Japan) and the results are presented in Table 2.

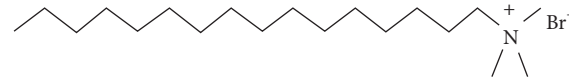

Figure 1: Structure of the surfactant cetyltrimethylammonium bromide.

XRD measurements of the raw and organoclay samples were performed using Rigaku 2200D/Max-IIIC (Rigaku Corporation, Tokyo, Japan) powder diffractometer equipment with CuKα radiation (λ = 1.5418 Å) source at 30 kV, 10 mA and at scan rate of 2° in min unit, and a scan range from 2° to 10°. X-ray diffraction patterns of the samples are given in Figure 2.

The XRD and the chemical analysis revealed that clay was a Na–montmorillonite (Na–Mt).

The cation-exchange capacity (CEC) of the clay is determined by the ammonium acetate method [32] as 107 meq/100 g. Cetyltrimethylammonium bromide (CTAB), a cationic surfactant also known as hexadecyltrimethylammonium bromide, was used as the modifier. With a long hydrocarbon chain, CTAB were purchased from Merck and used without further purification (Figure 1). All chemicals used in this study were obtained from Merck.

FT-IR spectra of all samples were run on a Perkin Elmer Model 1600 FT-IR spectrophotometer using KBr pellets.

Surface morphologies of the pristine montmorillonite and organoclay samples were examined by a Philips XL 30 SFEG model scanning electron microscope (SEM) operating at 24 kV.

The zeta potential measurements of solid particles in suspensions were carried out by using a Zeta Meter 3.0+ (Zeta-Meter, Inc., Staunton, VA, USA) at the unadjusted pHs.

The static contact angle measurement was performed using a CAM-101 optical contact angle analyzer (KSV Instruments, Finland). For this purpose, a pellet was prepared under 1.06 ton/cm^2 pressure, using 0.6 g organoclay sample. The contact angles were measured by using goniometer, which used a water drop of 6 μL and took Young-Laplace equation into account at solid-liquid interface.

2.2. Preparation of the Organoclays. The synthesis of surfactant modified montmorillonites was performed as in the following procedure: 50 g montmorillonite was first dispersed in distilled water and stirred for 10 h at stirring speed of 200–250 rpm to swell and to form homogeneous liquor, into which then a desired amount of cetyltrimethylammonium bromide (CTAB) was slowly added. The concentrations of surfactants were 0.5, 1.0, 1.5, and 2.0 times CEC of montmorillonite, respectively. The mixture was stirred for 1 h, then stirring was stopped and the resulting organomontmorillonite (OMt) was filtered and washed with distilled water for several times to remove excess salts, dried at 90°C, ground and sieved.

Table 3: The XRD results of the pristine montmorillonite and organoclay samples (unit/nm).

Sample	d_{001} (nm)	d_{002} (nm)
Mt	1.2620	—
0.5 CEC	1.8300	—
1.0 CEC	2.0066	—
1.5 CEC	2.8480	2.1480
2.0 CEC	4.2037	2.0066

3. Results and Discussion

3.1. Characterization of Organoclay Samples

3.1.1. XRD Investigations of Montmorillonite and Organoclay Samples. The modified clay samples by adsorption of cetyltrimethyl ammonium bromide (CTAB) based on cation exchange capacity (CEC) of clay were characterized by X-ray diffraction analysis (XRD), Fourier Transform Infrared (FTIR) spectrum. The XRD patterns are given in Figure 2. The XRD results of the pristine montmorillonite and organoclay samples are presented in Table 3. The $d_{(001)}$ (1.262 nm) of main peak indicates that the original sample is Na-montmorillonite. With an increase of surfactant concentration in the preparation solution, the basal spacing of the resultant organoclays increases in the following order: 1.83 nm (0.5 CEC-OMt), 2.0066 nm (1.0 CEC-OMt), 2.848 nm and 2.1480 nm (1.5 CEC-OMt), and 4.2037 nm and 2.066 nm (2.0 CEC-OMt), corresponding to lateral bilayer, pseudotrilayer, paraffin-type-monolayer and pseudotrilayer and paraffin-type-bilayer and pseudotrilayer, respectively. The single basal spacing of the organomontmorillonite with surfactant/CEC = 0.5 (0.5 CEC-OMt) is 1.83 nm. This peak corresponds to an interlayer opening of 0.87 nm (after subtraction of the silicate layer thickness value of 0.96 nm) and is the main reflection in the sample 0.5 CEC which is approximate to the height of lateral bilayer (0.81 nm). The organic ion arrangement can be considered as lateral bilayer. The possible arrangement model of the lateral bilayer is that the protrudent methyl inserts into cavity between organic cations or into the hexagonal hole of basal oxygen plane [13, 33, 34]. Consequently, the alkyl chains may come close together and arrange in LB model. So, the height of LB model depends on the height of the double layers of alkyl chains rather than that of the cation end of CTA^+.

The added surfactant/CEC ratio from 0.5 to 1 increases to the opening of the interlayers spaces by 0.1766 nm. The observed peak at 2.0066 nm for 1.0 CEC indicates that there is an interlayer spacing of 1.0466 nm in height. The height of the two layer of CTA^+ in a bilayer-mirror-image arrangement is just 1.02 nm which equals the interlayer spacing corresponding to the peak at 2.0066 nm. But, considering the repulsive force between cations, the probability for this kind of arrangement is little. Pseudotrilayer arrangement may explain well the basal reflection at 2.0066 nm. Brindley and Moll [35], Beneke and Lagaly [36] reported the arrangement model of alkyl chains with mutual interlocking, in which the parallel

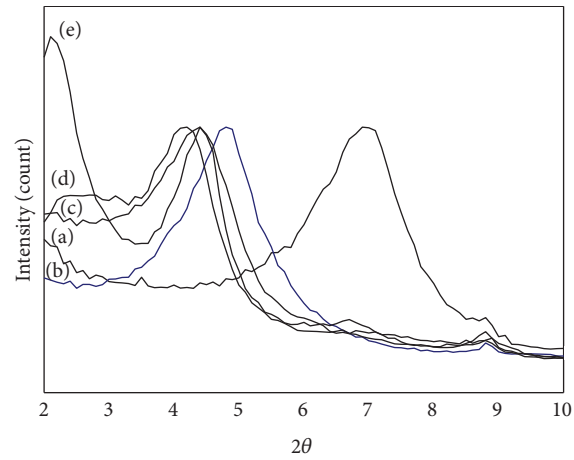

(a) Mt
(b) 0.5 CEC-OMt
(c) 1 CEC-OMt
(d) 1.5 CEC-OMt
(e) 2 CEC-OMt

Figure 2: XRD patterns of the pristine montmorillonite and the different organo-clays.

packing of the chains was presumed that a $-CH_2$ group of one chain laies between two such groups of neighbouring chains. In this case, the height of the bilayer with interlocking chains should be smaller than that without interlocking chains [37]. But, according to our results, the fact that interlayer basal spacing value of 1.0466 nm indicates the presence of CTA^+ ions connected with dispersive interactions to tail parts of CTA^+ ions apart from pseudotrilayer arrangement of CTA^+ ions. This result is supported by the increasing value of zeta potential (+25 mV).

The main peak of the organomontmorillonite with surfactant/CEC = 1.5 (1.5 CEC-OMt) has a basal spacing of 2.148 nm followed by a large shoulder centered at about 2.848 nm. This indicates a lack of the homogeneous interlayer opening due to the different interlayer expansions. The reason is that the amount of added surfactant is low compared to the CEC of the clay mineral and that not all charge balancing cations are replaced by the surfactant cations. Both nonexchanged inorganic cations (hydrated Na^+) and organic cations (cationic surfactant) are present, perhaps within the same interlamellar space [24].

The peak at the 2.148 nm (d_{002}) shows that the arrangement model of CTA^+ ions in the interlayer of montmorillonites is pseudotrilayer. The fact that the basal space distance is larger than the basal spacing distance required for pseudo trilayer shows that the CTA^+ ions connected with CTA^+ ions due to the dispersive interactions. The zeta potential measurements also support this result. The shoulder peak (d_{001}) on the left side of the d_{002} peak shows a new arrangement of CTA^+ ions between layers of clay other than the pseudo trilayer model. The maximum value of this peak (d_{001}) is 2.848 nm, and CTA^+ ions between the clay layers have settled with a paraffinic monolayer arrangement.

Table 4: Positions and assignments of the IR vibration bands observed in the range of 400–4000 cm^{-1}.

Assignment	Frequency, cm^{-1}				
	Mt	0.5 CEC	1.0 CEC	1.5 CEC	2.0 CEC
Structural OH stretching	3634	3633.09	3633.14	3629.92	3624.39
Symmetric OH stretching (ν_1)	3444	3435.98	3435.09	3434.57	3434.74
Asymmetric OH stretching (ν_3)	—	—	—	—	—
Asymmetric CH_2 stretching	—	2931.17	2924.2	2919.77	2918.98
Symmetric CH_2 stretching	—	2855.75	2851.49	2850.57	2850.29
H–O–H bending (ν_2)	1642	1640.09	1638.01	1637.21	1633.37
CH_2 scissoring	1478	1476	1474.03	1473.07	1472.98
	1442	1440.09	1438.01	1437.21	1433.37
Si–O stretching	1018.43	1000.38	1036	1029	1022
	1101	1088	914.73	918	914.73
CH_2 rocking	797.47	797.16	797.16	798.08	797.17
	779.18	779.43	778.43	779.81	778.80

The XRD patterns of 2.0 CEC-OMt show a well-organized structure, with a narrow first higher intensity peak at 4.2037 nm and with a second peak at 2.0066 nm corresponding to parafinic bilayer and pseudo trilayer arrangement, respectively. This indicates that the amount of added surfactant has a direct effect on the interlayer expansion of smectites. The surfactant chains lie parallel to each other in a paraffin-type structure at a certain angle with the silicate layers. For 2.0 CEC-OMt, the d_{001} basal spacing (4.2037 nm) corresponds to a configuration of C_{16} chains almost perpendicular to the clay layer [24]. A value of 4.2037 nm is obtained for a theoretical basal distance of OMt assuming a trans conformation of the chain in the interlamellar space.

In summary, by adding increasing amount of surfactant, several ranges of paraffin-like structures occur (i) <3 nm till 1.5 CEC and (ii) >4 nm after the CEC with highly ordered assembly. There is probably an intermediate configuration where the chains are not perpendicular to the layers with enough free lateral spaces allowing the chains to adopt different orientations leading to highest entropy. With the increase of the concentration of pillaring reagent, the stack density of organic cations in the interlayer space increases and the arrangement of organic cations changes. The heterogeneity of charge on various layers may be the crucial factor for different arrangements coexisting. Tamura and Nakazawa [38] proposed that the basal spacing of 3.98 nm should be attributed to the PB model and the *a* PB (between the alkyl chain and basal surface) was 30°. In the analogous study, Beneke and Lagaly [36] pointed out that long alkyl chain ($n > 16$) alkylammonium arranged in a paraffinic bilayer model and the basal spacing reached 4.0 nm. The occurrence of the basal spacing of 4.2037 nm in our study implies that CTA^+ ions should be arranged in the paraffinic bilayer model and the *a* PB > 30° [34]. The peak at 2.0066 nm corresponds to pseudo trilayer arrangement. On the other hand, the measurements of zeta potential support that there are bounded CTA^+ ions through dispersive interactions to the tails of CTA^+ ions in paraffinic bilayer arrangement between the clay layers.

3.1.2. Infrared Spectra of the Montmorillonite and Organoclay Samples. Vibrational spectroscopy has been extensively used for probing the conformation in amine chain assemblies. Infrared spectroscopic studies have led to detailed correlation of the spectra with structural features such as chain conformation, chain packing, and even specific conformational sequences [8, 39, 40].

Fourier Transform Infrared (FTIR) spectra of the previously dried samples were recorded on a Pelkin-Elmer Spectrum-One instrument. Each sample was finely ground with oven-dried spectroscopic grade KBr and pressed into a disc. All samples were oven-dried at 120°C to remove physisorbed water. Then, the spectra were recorded at resolution between 400 and 4000 cm^{-1}. The FTIR spectra of pristine clay and the modified clay samples by adsorption of cethyltrimethylammonium bromide (CTAB) based on cation exchange capacity (CEC) of clay are shown in Figure 3 and all the important absorption bands and their assignments are listed in Table 4. As shown in Figure 3, though the different OMts (Figure 3) shows the peaks of the pristine clay, new characteristic peaks appear at 2931.17 cm^{-1}–2855.75 cm^{-1}, at 2924.2 cm^{-1}–2851.49 cm^{-1} at 2919.77 cm^{-1}–2850.57 cm^{-1} and at 2918.98 cm^{-1}–2850.24 cm^{-1} corresponding to the $-CH_2$ asymmetric, (_as(CH_2)) and $-CH_2$ symmetric (_s(CH_2)) stretching vibrations for 0.5 CEC, 1.0 CEC, 1.5 CEC and 2.0 CEC, respectively [41]. These peaks absent in the IR spectrum of the pristine Mt indicate the incorporation (or the presence) of the surfactant in the different OMts. As the peaks are very narrow, we can compare the variation of their intensity instead of their peak area in order to estimate the increase of adsorbed amount of surfactant. The intensity increases with increasing initial surfactant content, indicating the intercalation of higher amount of surfactant in the montmorillonite with increasing initial amount. For CEC values between 0.5 and 1, the linear increase of the intensity with the amount of surfactant added is steeper than between 1 and 2 CEC. The first part, till 1 CEC, corresponds to a linear direct cationic exchange of the exchangeable Na^+ cation by the cationic surfactant. The second part, in

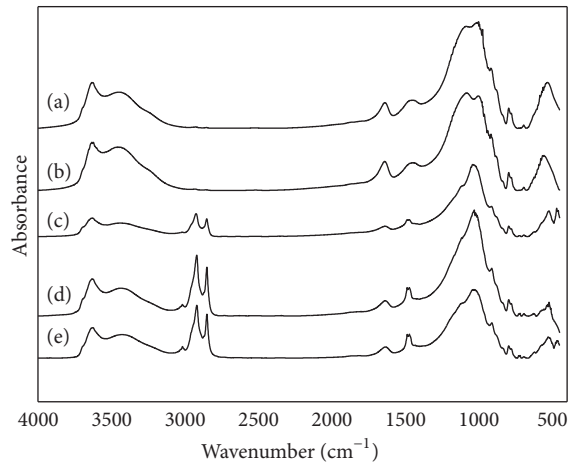

(a) Mt
(b) 0.5 CEC-OMt
(c) 1 CEC-OMt
(d) 1.5 CEC-OMt
(e) 2 CEC-OMt

Figure 3: FTIR spectra of the pristine montmorillonite and the different organoclays.

excess of the CEC, deviates from the previous linearity and corresponds to an adsorption of surfactant on the external surface, followed by adsorption in the interlamellar space, by lateral chain-chain surfactant interactions.

Previous studies [10, 42] indicated that the ordered conformation of the alkyl chains in the confined system showed a strong dependence on amine concentration and orientation. In relatively high concentration range, the confined amine chains adopt an essential all-trans-conformation and the frequency of the asymmetric CH_2 stretching absorption band locates at a relatively low frequency. However, in the relatively low amine concentration range, the frequency shifts significantly to higher frequency and the confined amine chains adopt a large number of gauche conformations. Only when the chains are highly ordered (all-trans-conformation), the narrow absorption bands appear around 2918 (_as(CH_2)) and 2850 cm^{-1} (_s(CH_2)) in the infrared spectrum. If conformational disorder is included in the chains, their frequencies shift upward, depending upon the average content of gauche conformers.

As shown in Figure 3 and Table 4 the frequency shifted significantly to low wavenumber, indicating more transconformational molecules introduced into alkyl chain with the increase of surfactant loading.

Kung and Hayes [10] figured out the relative shifts of $-CH_2$ vibrational energies can be used to assess the relative hydrophobic properties of the loaded surfactant, with lower energies (lower wave number) reflecting a more structured and hydrophobic environment. The results obtained in this study reflect that the degree of the hydrophobic properties may be increased with the increment of surfactant loading. At relatively high surfactant loading, most hydration cations were exchanged by surfactant cations, resulting in a decrease of the hydration water content and a surface property change from hydrophilic to hydrophobic. In this case, water molecules are difficult to be introduced into clay interlayer space and the gallery height is impossible to be expanded [40].

The infrared absorption bands between 1480 and 1440 cm^{-1}, due to the methylene scissoring modes, are quite similar to the methylene rocking modes at 800–700 cm^{-1} in the position and shape of the bands (shown in Figure 3). In the spectra of pristine Mt, doublets at 1478 and 1442 cm^{-1} corresponds to the scissoring modes and those at 797.47 and 779.18 cm^{-1} to the rocking modes, respectively. The splitting of the $-CH_2$ scissoring and rocking bands is due to the intermolecular interaction between the two adjacent hydrocarbon chains in a perpendicular orthorhombic subcell [43, 44] and further requires an all-trans-conformation for its detection [45]. As shown from Figure 3, when the alkyl intercalated into montmorillonite, a broad band at 1478 cm^{-1} splits with the increase of surfactant loading as described in the literature [15] for 1.0 CEC, 1.5 CEC, and 2.0 CEC. For the $-CH_2$ rocking modes, with the increase of surfactant loading, two well-resolved vibration bands at 797 and 778 cm^{-1} were observed, similar to $-CH_2$ scissoring. This phenomenon is similar to those descriptions in previous researches [46]. According to above results, it could be said that splitting of the methylene scissoring and rocking modes not only relates with surfactant loading, but also relates with the configuration of the used surfactants.

Spectral hydration features in montmorillonite have been attributed to the structural OH in the octahedral layer, water adsorbed on the clay external surfaces, and water adsorbed in the interlayer regions. The character of these interlayer water molecules is greatly dependent on the moisture level and the interlayer cation [40].

The spectra display more obvious absorption band at 3620 cm^{-1} due to the OH stretching vibrations of structural OH groups and the frequency is independent on the surfactant loading which is consistent with the result reported in the literature [40]. In the region of 3100–3500 cm^{-1}, the spectra show a broad band around 3400 cm^{-1} corresponding to the overlapping symmetric $\_\nu_1$ (H–O–H) and asymmetric $\_\nu_3$ (H–O–H) stretching vibrations, and a shoulder around 3250 cm^{-1} due to an overtone ($2\nu_2$) of the bending model [10, 24, 40]. As seen in Table 4, the frequency of the band around 3444 cm^{-1} gradually shifts to the lower frequency with the increase of surfactant loading. The H–O–H bending vibration shifts significantly from 1642 cm^{-1} (pristine Mt) to low frequency of 1640.09 cm^{-1} (0.5 CEC-OMt), of 1638.01 cm^{-1} (1.0 CEC-OMt), of 1637.21 cm^{-1} (1.5 CEC-OMt), and of 1633.37 cm^{-1} (2.0 CEC-OMt). When the surfactants intercalated into the gallery of montmorillonites, the water bounded directly to the hydrated cations was removed with the replacement of the hydrated cations by surfactant cations. Therefore, the detected absorption bands are mainly attributed to adsorbed water molecules especially at high surfactant loading. Simultaneously, with the intercalation of surfactants, the surface property of montmorillonite is modified; that is, the hydrophilic surface of montmorillonite

has been changed to hydrophobic. Hence, H_2O is not easy to be adsorbed by organomontmorillonite [40]. Zeta potential measurements support these results.

When the surfactant intercalated into interlayer space of montmorillonites, the frequency of the Si–O stretching band in the tetrahedral network was changed. As seen from Figure 3, for the pristine montmorillonite, the band in the region of 950–1100 cm^{-1} corresponding to stretching vibration of Si–O group splits into a sharp band at 1033 cm^{-1} with a shoulder around 1088 cm^{-1} attributed to perpendicular Si–O stretching [40]. However, for the organo-montmorillonites, the change of the band shape and its frequency strongly depends on the surfactant loading. As seen in Figure 3, frequencies of the Si–O stretching bands observed at the 1101 $cm^{-1}$and at the 1018,43 cm^{-1} for the pristine Mt shifted with a surfactant loading. For the organoclays prepared from CTAB with a low surfactant loading the shoulder at ca. 1101 cm^{-1} is markedly reduced. With the increase of surfactant loading, the shoulder band shifted to low frequency, from 1101 cm^{-1} to 1088 cm^{-1} for 0.5 OMt, to 914.73 cm^{-1} for 1.0 OMt. When further increasing the surfactant loading, the frequency almost kept unchanged for 1.5 CEC-OMt and 2.0 CEC-OMt (to 918 cm^{-1} for 1.5 OMt and to 914 cm^{-1} for 2.0 OMt). After the intercalation of CTAB, the band at the 1018.43 cm^{-1} shifted to 1000.38 cm^{-1}, to 1036 cm^{-1}, to 1029 $cm^{-1}$and to 1022 cm^{-1} for 0.5 CEC-OMt, 1.0 CEC-OMt, 1.5 CEC-OMt and 2.0 CEC-OMt, respectively. This is coincident with that reported in the previous studies [10, 47–50]. The intercalation of CTAB (as cation, or a neutral molecule) into the interlayer space is accompanied by a marked interlayer swelling, during which a perpendicular sorbate orientation is reached. In this way, the interlayer distance is markedly increased, the orientation of the SiO_4 tetrahedral is changed, most probably towards a better ordered arrangement and more marked manifestation of the perpendicular Si–O vibrations. Xi et al. [51] proposed that the significant changes in Si–O stretching band suggest that there is an interaction between the surfactant molecules and siloxane (Si–O) surface. Thus, the changes of Si–O stretching band are attributed to an increase of the interaction between the surfactant and silicate surfaces.

3.2. Zeta Potential and Contact Angle Measurements of the Montmorillonite and Organoclay Samples. The values of zeta potential and contact angle of pristine montmorillonite and organoclays were measured. The variation zeta potential and contact angel depending on CEC ratio are given in Figure 4. As shown from Figure 4, there are linear increase in the zeta potential values as it increased the CEC ratio and it reaches to maximum value at 2.0 CEC. The observed increase in the the contact angle values of organoclay samples by comparison pristine montmorillonite reaches to maximum value at 1.0 CEC, thereafter relative decrease observed in these values for 1.5 CEC and 2.0 CEC.

The value of zeta potential shifted to positive value with the increase of the CEC ratio. The significant increase appeared up to 1.0 CEC, then relative increase carried out for other CEC ratios. Depending on the contact angle value is

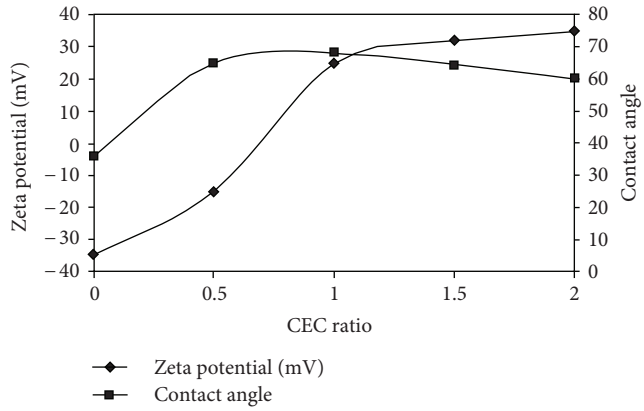

Figure 4: The variation of zeta potential and contact angle depend on surfactant loading.

quite low for pristine Mt, it can be said that diffusion trend of water to the spaces between the layers is extremely high, and water molecules penetrated to the basal area bond with silicate oxygen by hydrogen bonding. As a result, hydrated cations in a basal area improve wetting properties of the montmorillonite.

The values of zeta potential and contact angle in 0.5 OMt sample increased twice in respect of pristine montmorillonite.It was understood from these results that the interactions between CTA^+ ions and the negative centers on the montmorillonite surface occur through weak and electrostatic interactions and CTA^+ ions in basal space tend to orientate interval surface as parallel and lateral interactions appear as reciprocal. The increase in contact angle supports this result. Namely, CTA^+ ions tended as parallel and laterally interacted have negatively changed the wetting characteristic of clay and the existence tendency of water molecules in basal region. FTIR spectra (Figure 3) show that creating an effective dipole-dipole interaction and hydrogen bonding are trends of organoclay samples according to pristine Mt sample decreased.

The zeta potential value of 1.0 CEC-OMt samples has reached a very high and a positive value. In parallel, a significant increase in the value of contact angle has appeared. The conversion of zeta potential from negative value to positive value indicated that the orientation of CTA^+ ions at interface is changed from parallel to perpendicular. But the fact that the zeta potential value is greater than zero indicated the presence of dispersive interactions between parts of tails of the adsorbed CTA^+ ions in basal space of montmorillonite and of the attached CTA^+ ions partly as a horizontal. Despite the positive charge in the basal spaces of montmorillonite layers, it is a fact that the value of contact angle is significantly large (the changes of Si–O stretching band supports this result) showing that the tendency of diffusion of water is reduced by the hydrophobic tail parts of CTA^+ ions.

The considerable increase in the zeta potential value of 1.5 CEC-OMt sample has pointed completely vertical orientation. XRD observations (Figure 2) clearly indicate that formed structures similar to the situation at 1.0 CEC-OMt.

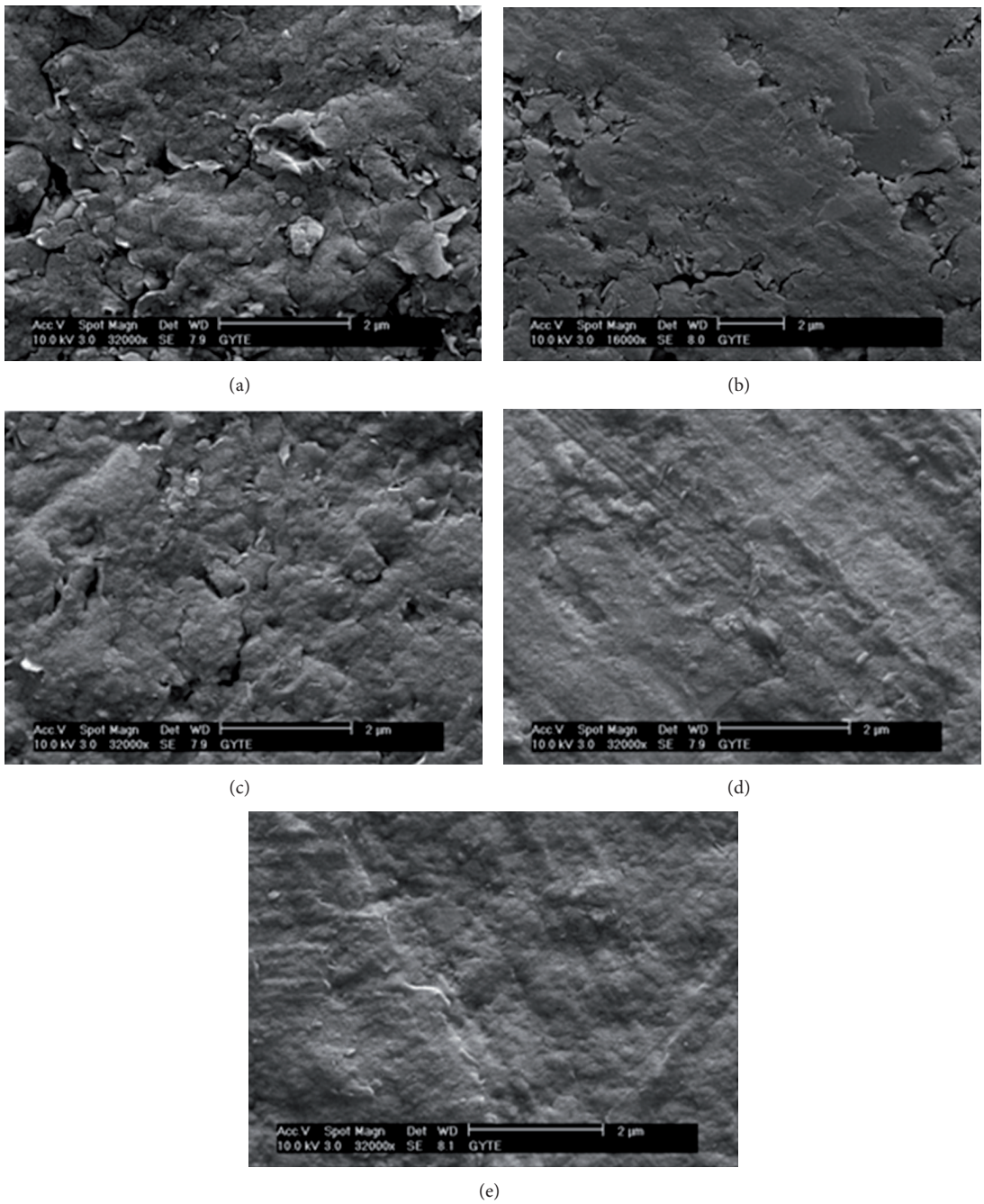

Figure 5: The SEM images of the pristine montmorillonite and the different organoclays (a) Mt, (b) 0.5 CEC-OMt, (c) 1.0 CEC-OMt, (d) 1.5 CEC-OMt, (e) 2.0 CEC-OMt.

Pseudotrilayer structure at 1.5 CEC-OMt sample reveals also the vertically oriented paraffinic monolayer structure depending on the increased concentration of CTA^+ ions. The electrostatic interactions due to high CTA^+ ion concentration at 1.5 CEC-OMt leads to emergence of paraffinic monolayer orientation primarily with the support of the vertical and horizontal dispersion interactions between the tails. Thereafter, the rest of the CTA^+ ions from the paraffinic oriented CTAB molecules leads to an adsorption of similar structure at 1.0 CEC-OMt sample.

It was seen that the measured zeta potential value in the case of 2.0 CEC-OMt is extremely large and the contact angle value was relatively low than that of the other samples. This situation has pointed to the transformation of some of CTA^+ ions between the layers of Mt from the paraffinic monolayer structure to the paraffinic bilayer structure. Extremely high and positive value of zeta potential and also the fact that the distance determined from the XRD measurements (Table 3) is relatively large expose the reciprocal semimicelle formation. Due to the requirement of being away from as possible

between similar charges this formation leads to a partial expansion at the basal distance. After this stage, decrease in concentration gradient leads to the transformation of the structure to pseudotrilayer structure.

3.3. SEM Analysis of the Montmorillonite and Organoclay Samples. SEM images of Mt and OMt samples to determine the surface morphology were taken and these images are given in Figure 5. In the SEM image of Mt sample some phase separations are seen, cracks and generally as a heterogeneous surface morphology. As seen in the SEM image of 0.5 CEC-OMt sample, the particles went to a more compact structure, increased tendency to aggregation and cracks and other defects are greatly reduced according to the Mt pattern. It can be said that compact structure occurs with the lateral interactions of the hydrophobic tails of CTAB on the taktoid surfaces. However, having particles lateral bilayer structure and the fact that the negative value of zeta potential (−15 mV) are considered as a reason for the occurred sharp cracks in the resulting morphology.

Unlike the case of 0.5 CEC-OMt, three-dimensional enlargements took place and structure reminiscent of pseudo-three-layer structures the spherical aggregates formed in the 1.0 CEC-OMt sample and the presence of fractures and faults are observed as a result of the presence of charged groups.

As it is evident from the XRD observations of 1.5 CEC-OMt sample, the spherical aggregates are seen as a result of the planar structures which reflected the structuring of paraffinic monolayer and pseudotrilayer of CTAB (it confirmed the presence of two different structuring).

The presence of paraffinic bilayer orientation in the case of 2.0 CEC-OMt is clearly seen in the topography of the material. In addition, spherical but dispersed relatively homogeneously, but also be seen the traces of mainly pseudo-triple layer orientation.

4. Conclusions

Systematically investigating the basal spacing evolution of OMt during the intercalation of CTAB can provide novel insight to the microstructures of organo clays. The intercalated CTAB will continue its rearrangement within the interlayer space which can lead to increase of basal spacing value. The interlayer distance of the montmorillonite (OMt) and the packing density of CTA^+ in the interlayer increases with increased amounts of adsorbed surfactant, as confirmed by XRD pattern. According to the obtained results from basal spaces in XRD patterns of organoclays, the organic ion possible arrangement model can be considered as lateral bilayer, pseudo-trilayer, paraffin-type monolayer and pseudo trilayer and paraffin-type bilayer and pseudo trilayer for 0.5, 1, 1.5, and 2.0 CEC, respectively. FTIR spectrum and contact angle measurements of pristine montmorillonite and organo clays indicated the incorporation of surfactant and the changing of hydrophility in the different OMts. This study demonstrates that not only the arrangement model of surfactant but also the morphology of organoclay strongly depends on the surfactant packing density within the montmorillonite interlayer space. In addition, it can be also proposed that the surface charge magnitude or its distribution on clay mineral might be an important factor for expansion characteristics of organoclay.

References

[1] S. A. Boyd, M. M. Mortland, and C. T. Chiou, "Sorption characteristics of organic compounds on hexadecyltrimethylammonium-Smectite," *Soil Science Society of America Journal*, vol. 52, no. 3, pp. 652–657, 1988.

[2] W. F. Jaynes and S. A. Boyd, "Clay mineral type and organic compound sorption by hexadecyltrimethlyammonium-exchanged clays," *Soil Science Society of America Journal*, vol. 55, no. 1, pp. 43–48, 1991.

[3] I. Dékány, A. Farkas, Z. Kiraly, E. Klumpp, and H. D. Narres, "Interlamellar adsorption of 1-pentanol from aqueous solution on hydrophobic clay mineral," *Colloids and Surfaces A*, vol. 119, no. 1, pp. 7–13, 1996.

[4] G. Sheng, X. Wang, S. Wu, and S. A. Boyd, "Enhanced sorption of organic contaminants by smectitic soils modified with a cationic surfactant," *Journal of Environmental Quality*, vol. 27, no. 4, pp. 806–814, 1998.

[5] B. Chen, L. Zhu, J. Zhu, and B. Xing, "Configurations of the bentonite-sorbed myristylpyridinium cation and their influences on the uptake of organic compounds," *Environmental Science and Technology*, vol. 39, no. 16, pp. 6093–6100, 2005.

[6] L. Z. Zhu, B. L. Chen, and X. Y. Shen, "Sorption of phenol, *p*-nitrophenol, and aniline to dual-cation organobentonites from water," *Environmental Science & Technology*, vol. 34, no. 3, pp. 468–475, 2000.

[7] B. K. G. Theng, R. H. Newman, and J. S. Whitton, "Characterization of an alkylammonium-montmorillonite-phenanthrene intercalation complex by carbon-13 nuclear magnetic resonance spectroscopy," *Clay Minerals*, vol. 33, no. 2-3, pp. 221–229, 1998.

[8] R. A. Vaia, R. K. Teukolsky, and E. P. Giannelis, "Interlayer structure and molecular environment of alkylammonium layered silicates," *Chemistry of Materials*, vol. 6, no. 7, pp. 1017–1022, 1994.

[9] G. Lagaly, "Characterization of clays by organic compounds," *Clay Minerals*, vol. 16, no. 1, pp. 1–21, 1981.

[10] K. H. S. Kung and K. F. Hayes, "Fourier transform infrared spectroscopic study of the adsorption of cetyltrimethylammonium bromide and cetylpyridinium chloride on silica," *Langmuir*, vol. 9, no. 1, pp. 263–267, 1993.

[11] L. Q. Wang, J. Liu, G. J. Exarhos, K. Y. Flanigan, and R. Bordia, "Conformation heterogeneity and mobility of surfactant molecules in intercalated clay minerals studied by solid-state NMR," *Journal of Physical Chemistry B*, vol. 104, no. 13, pp. 2810–2816, 2000.

[12] S. Y. Lee and S. J. Kim, "Expansion of smectite by hexadecyltrimethylammonium," *Clays and Clay Minerals*, vol. 50, no. 4, pp. 435–445, 2002.

[13] J. Zhu, H. He, J. Guo, D. Yang, and X. Xie, "Arrangement models of alkylammonium cations in the interlayer of $HDTMA^+$ pillared montmorillonites," *Chinese Science Bulletin*, vol. 48, no. 4, pp. 368–372, 2003.

[14] H. He, R. L. Frost, F. Deng, J. Zhu, X. Wen, and P. Yuan, "Conformation of surfactant molecules in the interlayer of montmorillonite studied by 13C MAS NMR," *Clays and Clay Minerals*, vol. 52, no. 3, pp. 350–356, 2004.

[15] J. Zhu, H. He, L. Zhu, X. Wen, and F. Deng, "Characterization of organic phases in the interlayer of montmorillonite using FTIR and 13C NMR," *Journal of Colloid and Interface Science*, vol. 286, no. 1, pp. 239–244, 2005.

[16] H. He, R. L. Frost, T. Bostrom et al., "Changes in the morphology of organoclays with HDTMA+ surfactant loading," *Applied Clay Science*, vol. 31, no. 3-4, pp. 262–271, 2006.

[17] J. Zhu, T. Wang, R. Zhu, F. Ge, P. Yuan, and H. He, "Expansion characteristics of organo montmorillonites during the intercalation, aging, drying and rehydration processes: effect of surfactant/CEC ratio," *Colloids and Surfaces A*, vol. 384, no. 1–3, pp. 401–407, 2011.

[18] D. Ovadyahu, S. Yariv, and I. Lapides, "Mechanochemical adsorption of phenol by TOT swelling clay minerals. I. Thermo-IR-spectroscopy and X-ray study," *Journal of Thermal Analysis and Calorimetry*, vol. 51, no. 2, pp. 415–430, 1998.

[19] J. Zhu, L. Zhu, R. Zhu, and B. Chen, "Microstructure of organobentonites in water and the effect of steric hindrance on the uptake of organic compounds," *Clays and Clay Minerals*, vol. 56, no. 2, pp. 144–154, 2008.

[20] C. C. Wang, L. C. Juang, C. K. Lee, T. C. Hsu, J. F. Lee, and H. P. Chao, "Effects of exchanged surfactant cations on the pore structure and adsorption characteristics of montmorillonite," *Journal of Colloid and Interface Science*, vol. 280, no. 1, pp. 27–35, 2004.

[21] L. Zampori, P. Gallo Stampino, G. Dotelli, D. Botta, I. Natali Sora, and M. Setti, "Interlayer expansion of dimethyl ditallowylammonium montmorillonite as a function of 2-chloroaniline adsorption," *Applied Clay Science*, vol. 41, no. 3-4, pp. 149–157, 2008.

[22] Q. Zhou, H. P. He, J. X. Zhu, W. Shen, R. L. Frost, and P. Yuan, "Mechanism of p-nitrophenol adsorption from aqueous solution by $HDTMA^+$-pillared montmorillonite-Implications for water purification," *Journal of Hazardous Materials*, vol. 154, no. 1–3, pp. 1025–1032, 2008.

[23] L. Zampori, P. G. Stampino, and G. Dotelli, "Adsorption of nitrobenzene and orthochlorophenol on dimethyl ditallowyl montmorillonite: a microstructural and thermodynamic study," *Applied Clay Science*, vol. 42, no. 3-4, pp. 605–610, 2009.

[24] T. Mandalia and F. Bergaya, "Organo clay mineral-melted polyolefin nanocomposites effect of surfactant/CEC ratio," *Journal of Physics and Chemistry of Solids*, vol. 67, no. 4, pp. 836–845, 2006.

[25] Y. Komori and K. Kuroda, "Layered silicate-polymer interlocation composites varieties in host materials and properties," in *Polymer-Clay Nanocomposites*, T. J. Pinnavaia and G. W. Beall, Eds., pp. 3–18, John Wiley & Sons, New York, NY, USA, 2001.

[26] E. Olewnik, K. Garman, and W. Czerwiński, "Thermal properties of new composites based on nanoclay, polyethylene and polypropylene," *Journal of Thermal Analysis and Calorimetry*, vol. 101, no. 1, pp. 323–329, 2010.

[27] H. Li, M. Eddaoudi, M. O'Keeffe, and O. M. Yaghi, "Design and synthesis of an exceptionally stable and highly porous metal-organic framework," *Nature*, vol. 402, no. 6759, pp. 276–279, 1999.

[28] K. R. Srinivasan and H. S. Fogler, "Use of inorgano-organoclays in the removal of priority pollutants from industrial wastewaters: adsorption of benzo(a)pyrene and chlorophenols from aqueous solutions," *Clays & Clay Minerals*, vol. 38, no. 3, pp. 287–293, 1990.

[29] P. X. Wu, Z. W. Liao, H. F. Zhang, and J. G. Guo, "Adsorption of phenol on inorganic-organic pillared montmorillonite in polluted water," *Environment International*, vol. 26, no. 5-6, pp. 401–407, 2001.

[30] A. Elmchaouri and R. Mahboub, "Effects of preadsorption of organic amine on Al-PILCs structures," *Colloids and Surfaces A*, vol. 259, no. 1–3, pp. 135–141, 2005.

[31] W. Xue, H. He, J. Zhu, and P. Yuan, "FTIR investigation of CTAB-Al-montmorillonite complexes," *Spectrochimica Acta—Part A*, vol. 67, no. 3-4, pp. 1030–1036, 2007.

[32] J. D. Rhoades, "Cation exchange capacity," in *Methods of Soil Analysis Part Chemical and Microbiological Properties*, p. 149, American Society of Agronomy/Soil Science Society of America, Madison, Wis, USA, 2nd edition, 1982.

[33] A. Vahedl-Faridi and S. Guggenheim, "Crystal structure of tetramethylammonium-exchanged vermiculite," *Clays and Clay Minerals*, vol. 45, no. 6, pp. 859–866, 1997.

[34] H. Heinz, R. A. Vaia, R. Krishnamoorti, and B. L. Farmer, "Self-assembly of alkylammonium chains on montmorillonite: effect of chain length, head group structure, and cation exchange capacity," *Chemistry of Materials*, vol. 19, no. 1, pp. 59–68, 2007.

[35] G. W. Brindley and W. F. Moll, "Complexes of natural and synthetic. Ca-montmorillonites with fatty acids," *American Mineralogist*, vol. 50, pp. 1355–1370, 1965.

[36] K. Beneke and G. Lagaly, "The brittle mica-like $KNiAsO_4$ and its organic derivatives," *Clay Minerals*, vol. 17, no. 2, pp. 175–183, 1982.

[37] J. H. Choy, S. Y. Kwak, Y. S. Han, and B. W. Kim, "New organo-montmorillonite complexes with hydrophobic and hydrophilic functions," *Materials Letters*, vol. 33, no. 3-4, pp. 143–147, 1997.

[38] K. Tamura and H. Nakazawa, "Intercalation of N-alkyltrimethylammonium into swelling fluoro-mica," *Clays and Clay Minerals*, vol. 44, no. 4, pp. 501–505, 1996.

[39] N. V. Venkataraman and S. Vasudevan, "Conformation of methylene chains in an intercalated surfactant bilayer," *Journal of Physical Chemistry B*, vol. 105, no. 9, pp. 1805–1812, 2001.

[40] Y. Ma, J. Zhu, H. He, P. Yuan, W. Shen, and D. Liu, "Infrared investigation of organo-montmorillonites prepared from different surfactants," *Spectrochimica Acta—Part A*, vol. 76, no. 2, pp. 122–129, 2010.

[41] V. C. Farmer, *The Infra Red Spectra of Clay Minerals*, Mineralogical Society, London, UK, 1974.

[42] H. Hongping, F. L. Ray, and Z. Jianxi, "Infrared study of $HDTMA^+$ intercalated montmorillonite," *Spectrochimica Acta—Part A*, vol. 60, no. 12, pp. 2853–2859, 2004.

[43] R. G. Snyder, "Vibrational correlation splitting and chain packing for the crystalline *n*-alkanes," *The Journal of Chemical Physics*, vol. 71, no. 8, pp. 3229–3235, 1979.

[44] H. L. Casal, H. H. Mantsch, D. G. Cameron, and R. G. Snyder, "Interchain vibrational coupling in phase II (hexagonal) *n*-alkanes," *The Journal of Chemical Physics*, vol. 77, no. 6, pp. 2825–2830, 1982.

[45] C. R. Flach, A. Gericke, and R. Mendelsohn, "Quantitative determination of molecular chain tilt angles in monolayer films at the air/water interface: infrared reflection/absorption spectroscopy of behenic acid methyl ester," *Journal of Physical Chemistry B*, vol. 101, no. 1, pp. 58–65, 1997.

[46] Y. Li and H. Ishida, "Concentration-dependent conformation of alkyl tail in the nanoconfined space: hexadecylamine in the silicate galleries," *Langmuir*, vol. 19, no. 6, pp. 2479–2484, 2003.

[47] J. T. Kloprogge and R. L. Frost, "Infrared emission spectroscopy of Al-pillared beidellite," *Applied Clay Science*, vol. 15, no. 5-6, pp. 431–445, 1999.

[48] S. Acemana, N. Lahav, and S. Yariv, "A thermo-FTIR-spectroscopy analysis of Al-pillared smectites differing in source of charge, in KBr disks," *Thermochimica Acta*, vol. 340-341, pp. 349–366, 1999.

[49] J. T. Kloprogge, E. Booy, J. B. H. Jansen, and J. W. Geus, "The effect of thermal treatment on the properties of hydroxy-Al and hydroxy-Ga pillared montmorillonite and beidellite," *Clay Minerals*, vol. 29, no. 2, pp. 153–167, 1994.

[50] L. Li, X. Liu, Y. Ge, R. Xu, J. Rocha, and J. Klinowski, "Structural studies of pillared saponite," *Journal of Physical Chemistry*, vol. 97, no. 40, pp. 10389–10393, 1993.

[51] Y. Xi, Z. Ding, H. He, and R. L. Frost, "Infrared spectroscopy of organoclays synthesized with the surfactant octadecyltrimethylammonium bromide," *Spectrochimica Acta—Part A*, vol. 61, no. 3, pp. 515–525, 2005.